Tunneling current and emission spectrum of a single-electron transistor under optical pumping

David M.-T. Kuo[1] and Yia-Chung Chang[2]
[1]*Department of Electrical Engineering, National Central University, Chung-Li, Taiwan, Republic of China*
[2]*Department of Physics, University of Illinois at Urbana-Champaign, Urbana, Illinois 61801, USA*
(Received 15 March 2005; revised manuscript received 1 June 2005; published 18 August 2005)

Theoretical studies of the tunneling current and emission spectrum of a single electron transistor (SET) under optical pumping are presented. The calculation is performed via Keldysh Green's function method within the Anderson model with two energy levels. It is found that holes in the quantum dot (QD) created by optical pumping lead to new channels for the electron tunneling from emitter to collector. As a consequence, an electron can tunnel through the QD via additional channels, characterized by the exciton, trion, and biexciton states. It is found that the tunneling current as a function of the gate voltage displays a series of sharp peaks and the spacing between these peaks can be used to determine the exciton binding energy as well as the electron–electron Coulomb repulsion energy. In addition, we show that the single-photon emission associated with the electron-hole recombination in the exciton complexes formed in the QD can be controlled both electrically and optically.

DOI: 10.1103/PhysRevB.72.085334 PACS number(s): 73.63.Kv, 73.21.La, 73.23.Hk, 78.67.Hc

I. INTRODUCTION

The tunneling current characteristics of a single electron transistor (SET) have been extensively studied and interesting physical phenomena, such as Coulomb blockade and Kondo effect have been found.[1–7] The main structure of a SET consists of three electrodes (source, drain, and gate) and the active region consists of one or more quantum dots (QDs). The tunneling current of a SET is sensitive to the size of the QD. The charging energy, ΔU, is typically larger than the energy level spacing, ΔE, caused by the quantum confinement in large QDs. Consequently, the tunneling current displays a periodic Coulomb oscillation with respect to the gate voltage. This feature of periodic Coulomb oscillation is a consequence of homogeneity of ΔU and negligible ΔE. However, such a Coulomb oscillation was observed only at very low temperature due to the small charging energy. Note that the charging energy must be greater than the thermal energy and tunneling rate multiplied by $\hbar$ in order for a SET to operate properly. For application in high temperature SETs, nanoscale QDs with large charging energy are desired.

To date two major kinds of nanoscale QDs have been used to construct SETs: the Si/Ge QDs and the InAs/GaAs self-assembled quantum dots (SAQDs). Silicon (Si) or germanium (Ge) QDs can be miniaturized to reach nanometer scale with advanced fabrication technology. Nanoscale Si/Ge SETs typically display nonperiodic Coulomb oscillations at room temperatures,[8–11] as a result of the large charging energy (ΔU) and the unequally spaced values of ΔE, which are comparable to ΔU. Even though Si/Ge SETs can operate at room temperatures, it is difficult to gain full understanding of their tunneling current characteristics because of the multivalleyed nature of Si/Ge and the unknown $Si/Ge\text{-}SiO_2$ interface properties. Furthermore, the electron-hole recombination rate in Si/Ge QDs is not large enough for useful application in optoelectronics, since Si and Ge are indirect-band-gap semiconductors.[12]

The InAs/GaAs SAQDs, on the other hand, are better understood, and because InAs is a direct-band-gap semiconductor, SETs constructed from InAs/GaAs SAQDs can have useful application in optoelectronic devices such as single-photon generators and single-photon detectors. Recently, InAs/GaAs self-assembled quantum dot (SAQD) embedded in a *p-n* junction has been employed to generate single-photon emission for application in quantum cryptography.[13–15] Another way to achieve single-photon generation is to use isolated SAQD with optical pumping. Such studies have received a great deal of attention recently.[16–21] The spontaneous emission spectrum of a QD typically exhibits coexisting sharp emission peaks, which have been attributed to the electron-hole recombination in the exciton, trion, and biexciton formed in the QD. The antibunching feature of the emitted single photon in this kind of device has been demonstrated.[13,14] In addition, gate electrodes have been used in some experiments to manipulate the emission spectrum.[22–24]

Many theoretical efforts based on the Anderson model and Keldysh-Green's function method have been devoted to the studies of transport properties of SETs, including the dc and ac tunneling current.[5–7] The studies on the ac tunneling current of SET mainly focus on the photon-side band phenomena caused by the microwave pumping[5,7] via intraband excitation. Apart from photon-side bands, some interesting photon-assisted transport properties such as superradiance in electric current through double QDs embedded in a *p-n* junction and coherent population trapping in mesoscopic systems have been discussed in the review article by Brandes.[25] Only a handful of theoretical studies considered the optical properties of SETs. Recently, we have studied the intraband transitions of SETs made of InAs/GaAs SAQDs for application as an infrared photodetector with operating wavelength near 10 μm.[26,27] On the other hand, the interband transitions in a QD have been adopted frequently to realize single-photon generation. Theoretical studies of the electronically driven single-photon generator (SPG) have been reported,[28,29] whereas theoretical studies on optically pumped SETs are still lacking. It is the purpose of this paper to provide a theoretical analysis for such a system. Furthermore, the mea-

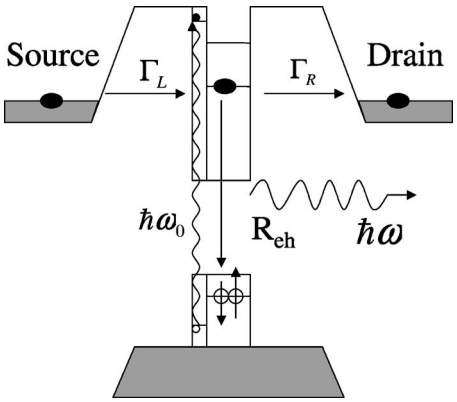

FIG. 1. Schematic diagram of a single electron transistor under optical pumping. Γ_L and Γ_R denote, respectively, the tunneling rate for electrons in the QD to the source and drain electrodes. R_{eh} denotes the electron-hole recombination rate. The vertical wavy line indicates the optical pumping, and the horizontal wavy line indicates the single-photon emission.

surement of exciton binding energy in a QD remains illusive, since in a typical photoluminescence measurement or the emission spectrum of a single QD, one can only observe the exciton recombination, but not the free electron-hole recombination. The exciton binding energy is an important physical quantity as it provides information about the effective dielectric constant and the charge distribution of electron and hole in the QD. In our current theoretical study, we will show that via the measurement of the tunneling current of an SET made of a nanoscale QD under optical pumping one can determine the exciton binding energy of a QD unambiguously.

The schematic diagram for the SET system considered is shown in Fig. 1. Here a nanoscale QD is embedded in an *n-i-n* junction. This is different from the electrically driven SPG, where a QD is embedded in a *p-n* junction. Therefore, the physical process considered here is also quite different. Using optical pumping to create electron-hole pairs in the SET, one cannot only electrically manipulate the single-photon emission spectrum arising from exciton complexes in the QD, but also optically control the tunneling current of the SET. In this paper, we will consider both the hole-assisted tunneling current due to optical pumping and the electrode-controlled spontaneous emission spectrum.

Our calculation is based on the Keldysh-Green's function approach[30] within the Anderson model for a two-level system. An effective-mass model, which takes into account the anisotropy and inhomogeneity, is used to estimate the interparticle Coulomb energies. We find that the optical excitation creates holes in the QD, which provide new channels (via the electron-hole interaction) for the electron to tunnel from the emitter to the collector. As a consequence, an electron can tunnel through the QD via four additional channels, characterized by the exciton, positive trion, negative trion, and biexciton states. Each additional channel can generate a new plateau (or oscillatory peaks) in the tunneling current characteristics in addition to the typical plateau (or peaks) caused by the Coulomb blockade effect. This gives rise to a rich tunneling current characteristic and it can be used to determine the exciton binding energy.

This paper is organized as follows. In Sec. II, we derive the tunneling current of SET under optical pumping. In Sec. III, we calculate the polarization needed for describing the spontaneous emission spectrum. In Sec. IV, we present calculations of the interparticle Coulomb interactions within a simple but realistic effective-mass model. In Sec. V, we discuss the results of our numerical calculations on the tunneling current and spontaneous emission spectrum and demonstrate that the exciton binding energy can be extracted via the measurement of tunneling current. Finally, a summary and concluding remarks are presented in Sec. VI.

II. TUNNELING CURRENT

The system of interest is shown in Fig. 1, which consists of a single InAs/GaAs self-assembled quantum dot (SAQD) sandwiched between two *n*-doped GaAs leads. Electrons are allowed to tunnel from the left lead (emitter) to the right lead (collector) under the influence of an optical field. The Hamiltonian for the system is given by

$$
\begin{aligned}
H = & \sum_{\sigma,i=e,h} E_i d^\dagger_{i,\sigma} d_{i,\sigma} + \sum_{\mathbf{k},\sigma;\ell=L,R} \epsilon_{\mathbf{k}} c^\dagger_{\mathbf{k},\sigma;\ell} c_{\mathbf{k},\sigma;\ell} \\
& + \sum_{\ell=L,R;k,\sigma} (V_{\mathbf{k},\sigma;\ell} c^\dagger_{\mathbf{k},\sigma;\ell} d_{e,\sigma} + V^\dagger_{\mathbf{k},\sigma;\ell} d^\dagger_{e,\sigma} c_{\mathbf{k},\sigma;\ell}) \\
& + \sum_{\mathbf{k},\sigma} (\lambda_0 e^{i\omega_0 t} b_{e,\mathbf{k},\sigma} b_{h,\mathbf{k},-\sigma} + \lambda_0^\dagger e^{-\omega_0 t} b^\dagger_{h,\mathbf{k},-\sigma} b^\dagger_{e,\mathbf{k},\sigma}) \\
& + \sum_{i,\mathbf{k},\mathbf{q},\sigma} (g_{i,\mathbf{q}} A b^\dagger_{i,\mathbf{k},\sigma} d_{i,\sigma} + g^\dagger_{i,\mathbf{q}} A^\dagger d^\dagger_{i,\sigma} b_{i,\mathbf{k},\sigma}) \\
& + \sum_{\mathbf{Q}} (\lambda e^{i\omega t} a^\dagger d_{e,\sigma} d_{h,-\sigma} + \lambda^\dagger e^{-i\omega t} a d^\dagger_{h,-\sigma} d^\dagger_{e,\sigma}), \qquad (1)
\end{aligned}
$$

where the first term describes electrons in the QD. We assume that the quantum confinement effect is strong for the small InAs QD considered here. Therefore, the energy spacings between the ground state and the first excited state for electrons and holes, ΔE_e and ΔE_h, are much larger than the thermal energy, $k_B T$, where k_B and T denote the Boltzmann constant and temperature. Only the ground state levels for electrons and holes, E_e and E_h, are considered in the first term. The second term describes the kinetic energies of free carriers in the electrodes. Note that in the current setup, the gate electrode does not provide any carriers, but merely controls the energy levels of the QD. The third term describes the coupling between the QD and the leads. Note that only the conduction band of QD is coupled with the electrodes. The fourth term describes the interband optical pumping with a frequency ω_0, which is in resonance with the transition energy for an electron-hole pair in the wetting layer. We treat the electromagnetic field as a semiclassical field. The fifth term describes the optical phonon assisted process for electrons in the wetting layer to relax into the InAs QD. The last term describes the coupling of the QD with the electromagnetic field of frequency ω. $\lambda \equiv -\mu_r \mathcal{E}$ is the Rabi frequency, where $\mu_r = \langle f|\mathbf{r}|\mathbf{i}\rangle$ is the matrix element for the optical transition and $\mathcal{E}$ is electric field per photon. $a^\dagger(A^\dagger)$ and $a(A)$ denote the creation and annihilation operators of a photon (phonon), respectively.

Due to the large strain-induced splitting between the heavy-hole and light-hole bands for typical QDs, we only have to consider the heavy-hole band (with $J_z=\pm 3/2$) and ignore its coupling with light-hole band caused by the QD potential. Thus, we can treat the heavy hole as a spin-1/2 particle with $\sigma=\downarrow,\uparrow$ representing $J_z=\pm 3/2$. This treatment is convenient for algebraic manipulations in the calculation of Green's functions. Because the effect of interparticle Coulomb interactions is significant in small semiconductor QDs, we take into account the electron Coulomb interactions and electron-hole Coulomb interactions by adding the following terms

$$H_I=\sum_{i,\sigma} U_{i,i} d_{i,\sigma}^{\dagger} d_{i,\sigma} d_{i,-\sigma}^{\dagger} d_{i,-\sigma} + \sum_{i\neq j;\sigma,\sigma'} U_{i,j} d_{i,\sigma}^{\dagger} d_{i,\sigma} d_{j,-\sigma}^{\dagger} d_{j,-\sigma}, \tag{2}$$

where $d_{i,\sigma}^{\dagger}$ and $d_{i,\sigma}$ are creation and annihilation operators for particles with spin σ in the ith energy level of the QD. Once the Hamiltonian is constructed, the tunneling current of SET can be calculated via the Keldysh-Green's function method.[7] We obtain the tunneling current through a single dot (see Appendix A):

$$J=\frac{-2e}{\hbar}\int \frac{d\epsilon}{2\pi}[f_L(\epsilon-\mu_L)-f_R(\epsilon-\mu_R)] \times \frac{\Gamma_L(\epsilon)\Gamma_R(\epsilon)}{\Gamma_L(\epsilon)+\Gamma_R(\epsilon)} Im G_{e,\sigma}^{r}(\epsilon), \tag{3}$$

where $f_L(\epsilon)$ and $f_R(\epsilon)$ are the Fermi distribution function for the source and drain electrodes, respectively. The chemical potential difference between these two electrodes is related to the applied bias via $\mu_L-\mu_R=eV_a$. $\Gamma_L(\epsilon)$ and $\Gamma_R(\epsilon)$ denote the tunneling rates from the QD to the left (source) and right (drain) electrodes, respectively. For simplicity, these tunneling rates will be assumed energy and bias independent. Therefore, the calculation of tunneling current is entirely determined by the spectral function $A=Im G_{e,\sigma}^{r}(\epsilon)$, which is the imaginary part of the retarded Green's function $G_{e,\sigma}^{r}(\epsilon)$. Equation (3) is obtained provided that the condition $\Gamma_{L(R)} \gg \gamma_{e,c}$ and $\Gamma_{L(R)} \gg R_{eh}$ are satisfied, where $\gamma_{e,c}$ is the captured rate of electrons. Because of the phonon bottleneck effect, we expect the rate for the electron to relax from the wetting layer to the QD is small. Thus, we have ignored the terms involving phonons in the calculation of the tunneling current. Besides, photon current has also been neglected, since the electron-hole recombination rate, R_{eh} is much smaller than the tunneling rates.

The retarded Green's function, $G_{e,\sigma}^{r}(\epsilon)$, can be obtained by the equation of motion of $G_{e,\sigma}^{r}(t)=-i\theta(t)\langle[d_{e,\sigma}(t), d_{e,\sigma}^{\dagger}(0)]\rangle$, where $\theta(t)$ is a step function. The curly brackets represent the anticommutator and the bracket $\langle\ldots\rangle$ denotes the thermal average. The Fourier transform of $G_{e,\sigma}^{r}(t)$ is given by

$$G_{e,\sigma}^{r}(\epsilon)=\int_{-\infty}^{\infty} dt G_{e,\sigma}^{r}(t) e^{i(\epsilon+i\eta)t} \tag{4}$$

with η being a positive infinitesimal number. $G_{e,\sigma}^{r}$ is the full Green's function, which includes all types of interactions. Given the conditions $\Gamma_{L(R)} \gg \gamma_{e,c}$ and $\Gamma_{L(R)} \gg R_{eh}$, we can drop the fifth and the last term of the Hamiltonian in the calculation of $G_{e,\sigma}^{r}(\epsilon)$. To solve $G_{e,\sigma}^{r}(\epsilon)$, we consider only the lowest order coupling between the electrodes and the QD. The equation of motion for $G_{e,\sigma}^{r}(t)$ leads to

$$\left(\epsilon-E_e+i\frac{\Gamma_e}{2}\right)G_{e,\sigma}^{r}(\epsilon) = 1+U_e G_{ee}^{r}(\epsilon)-U_{eh}[G_{eh,1}^{r}(\epsilon)+G_{eh2}^{r}(\epsilon)], \tag{5}$$

where the two particle Green's functions, $G_{ee}^{r}(\epsilon)$, $G_{eh1}^{r}(\epsilon)$, and $G_{eh,2}^{r}(\epsilon)$ arise from the particle correlation and they satisfy

$$\left(\epsilon-(E_e+U_e)+i\frac{\Gamma_e}{2}\right)G_{ee}^{r}(\epsilon) = N_{e,-\sigma}-U_{eh}[G_{ehe1}^{r}(\epsilon)+G_{ehe2}^{r}(\epsilon)], \tag{6}$$

$$\left(\epsilon-(E_e-U_{eh})+i\frac{\Gamma_e}{2}\right)G_{eh1}^{r}(\epsilon) = n_{h,\sigma}+U_e G_{ehe1}^{r}(\epsilon)-U_{eh}G_{ehh}^{r}(\epsilon), \tag{7}$$

and

$$\left(\epsilon-(E_e-U_{eh})+i\frac{\Gamma_e}{2}\right)G_{eh2}^{r}(\epsilon) = n_{h,-\sigma}+U_e G_{ehe2}^{r}(\epsilon)-U_{eh}G_{ehh}^{r}(\epsilon). \tag{8}$$

$N_{e,-\sigma}$, $n_{h,\sigma}$ and $n_{h,-\sigma}$ in Eqs. (6)–(8) denote the steady-state electron and hole occupation numbers. The two-particle Green's functions are coupled with the three-particle Green's functions defined as $G_{ehe1}^{r}(\epsilon)=\langle N_{e,-\sigma}n_{h,\sigma}d_{e,\sigma}, d_{e,\sigma}^{\dagger}\rangle$, $G_{ehe2}^{r}(\epsilon)=\langle N_{e,-\sigma}n_{h,-\sigma}d_{e,\sigma}, d_{e,\sigma}^{\dagger}\rangle$ and $G_{ehh}^{r}(\epsilon)=\langle n_{h,-\sigma}n_{h,\sigma}d_{e,\sigma}, d_{e,\sigma}^{\dagger}\rangle$. The equations of motion of the three-particle Green's functions will lead to coupling with the four-particle Green's functions (two electrons and two holes), where the hierarchy terminates. Thus, these three-particle Green's functions can be expressed in the following closed form

$$G_{ehe1}^{r}(\epsilon)=N_{e,-\sigma}n_{h,\sigma}\left(\frac{1-n_{h,-\sigma}}{\epsilon-(E_e+U_e-U_{eh})+i\frac{\Gamma_e}{2}} + \frac{n_{h,-\sigma}}{\epsilon-(E_e+U_e-2U_{eh})+i\frac{\Gamma_e}{2}}\right), \tag{9}$$

$$G^r_{ehe2}(\epsilon) = N_{e,-\sigma} n_{h,-\sigma} \left(\frac{1 - n_{h,\sigma}}{\epsilon - (E_e + U_e - U_{eh}) + i\frac{\Gamma_e}{2}} + \frac{n_{h,\sigma}}{\epsilon - (E_e + U_e - 2U_{eh}) + i\frac{\Gamma_e}{2}} \right), \quad (10)$$

and

$$G^r_{ehh}(\epsilon) = n_{h,-\sigma} n_{h,\sigma} \left(\frac{1 - N_{e,-\sigma}}{\epsilon - (E_e - 2U_{eh}) + i\frac{\Gamma_e}{2}} + \frac{N_{e,-\sigma}}{\epsilon - (E_e - 2U_{eh} + U_e) + i\frac{\Gamma_e}{2}} \right). \quad (11)$$

Equations (9) and (10) describe the mixed amplitudes for the propagation of an electron either in the presence of another electron (with opposite spin) plus one hole, or another electron plus two holes. Equation (11) describes the mixed amplitudes for the propagation of an electron either in the presence of two holes, or two holes plus another electron. Substituting Eqs. (9)–(11) into Eqs. (7) and (8), we obtain, after some algebras, the retarded Green's function of Eq. (3):

$$\begin{aligned} G^r_{e,\sigma}(\epsilon) = (1 - N_{e,-\sigma}) & \left(\frac{1 - (n_{h,\sigma} + n_{h,-\sigma}) + n_{h,\sigma} n_{h,-\sigma}}{\epsilon - E_e + i\frac{\Gamma_e}{2}} + \frac{n_{h,\sigma} + n_{h,-\sigma} - 2n_{h,\sigma} n_{h,-\sigma}}{\epsilon - E_e + U_{eh} + i\frac{\Gamma_e}{2}} + \frac{n_{h,\sigma} n_{h,-\sigma}}{\epsilon - E_e + 2U_{eh} + i\frac{\Gamma_e}{2}} \right) \\ & + N_{e,-\sigma} \left(\frac{1 - (n_{h,\sigma} + n_{h,-\sigma}) + n_{h,\sigma} n_{h,-\sigma}}{\epsilon - E_e - U_e + i\frac{\Gamma_e}{2}} + \frac{n_{h,\sigma} + n_{h,-\sigma} - 2n_{h,\sigma} n_{h,-\sigma}}{\epsilon - E_e - U_e + U_{eh} + i\frac{\Gamma_e}{2}} + \frac{n_{h,\sigma} n_{h,-\sigma}}{\epsilon - E_e - U_e + 2U_{eh} + i\frac{\Gamma_e}{2}} \right), \end{aligned} \quad (12)$$

where $G^r_{e,\sigma}(\epsilon)$ contains an admixture of six possible configurations in which a given electron can propagate. These configurations are: empty state, one-hole state, two-hole state, one-electron state, one-electron plus one-hole state, and one-electron plus two-hole state. In Eq. (12), Γ_e is the electron tunneling rate $\Gamma_e \equiv \Gamma_L + \Gamma_R$. The particle correlation has not been included in the tunneling rates of Eq. (12). Such approximation has been known to be adequate for describing the Coulomb blockade effect, but not the Kondo effect. The electron occupation number of the QD can be solved self-consistently via the relation

$$N_{e,\sigma} = -\int \frac{d\epsilon}{\pi} \frac{\Gamma_L f_L(\epsilon) + \Gamma_R f_R(\epsilon)}{\Gamma_L + \Gamma_R} Im G^r_{e,\sigma}(\epsilon). \quad (13)$$

$N_{e,\sigma}$ is limited to the region $0 \leqslant N_{e,\sigma} \leqslant 1$. Equation (13) indicates that the electron occupation numbers of the QD, $N_{e,-\sigma}$ and $N_{e,\sigma}$, are primarily determined by the tunneling process. To obtain the electron and hole occupation numbers ($n_{e,-\sigma} = n_{e,\sigma}$ and $n_{h,-\sigma} = n_{h,\sigma}$) arising from the optical pumping, we solve the rate equations (see Appendix B) and obtain

$$n_e = n_{e,-\sigma} = n_{e,\sigma} = \frac{\gamma_{e,c} N_{e,\mathbf{k}} (1 - N_e)}{\gamma_{e,c} N_{e,\mathbf{k}} + R_{eh} n_h + \Gamma_e}, \quad (14)$$

and

$$n_h = n_{h,-\sigma} = n_{h,\sigma} = \frac{\gamma_{h,c} N_{h,\mathbf{k}}}{\gamma_{h,c} N_{h,\mathbf{k}} + R_{eh}(n_e + N_e) + \Gamma_{h,s}}, \quad (15)$$

where $\gamma_{e(h),c}$ and $N_{e(h),\mathbf{k}}$ denote the captured rate for electrons (holes) from the wetting layer to the QD and the occupation number of electrons (holes) in the wetting layer. See Eqs. (B5) and (B6), $N_{e(h),\mathbf{k}}$ is a linear function of p_{exc} for low pumping intensity and small $\gamma_{e(h),c}$. $\Gamma_{h,s}$ denotes the nonradiative recombination rate for holes in the QD. Because $\gamma_{e,c} N_{e,\mathbf{k}} / \Gamma_e \ll 1$, n_e has been neglected in Eq. (12).

III. SPONTANEOUS EMISSION SPECTRUM

When electrons and holes appear in the QD, their recombination leads to single-photon emission. The optical polarization of the emitted photon depends on the spin polarization of the electrons. An electron with spin +1/2 (−1/2) can recombine with a heavy hole of angular momentum +3/2 (−3/2) to emit a circularly (σ^+ *or* σ^-) polarized photon. In some experiments, up to four coexisting peaks (associated with exciton, negative trion, positive trion, and biexciton) have been observed in the emission spectrum.[16–18] The emission process is described by the last term in the Hamiltonian given in Eq. (1). The bias-dependent emission spectrum can be obtained by finding the nondiagonal lesser Green's function at nonequal time.[7] To simplify the problem, we assume that the applied bias is large enough to create the biexciton state (two electrons and two holes) in the QD.

With the above assumption, polarization $P(\omega) = G^<_{eh}(\omega)$ can be calculated by the equal-time Keldysh-Green function, $G^<_{eh} < (t,t) = -i\langle a^\dagger(t) d_{h,-\sigma}(t) d_{e,\sigma}(t) \rangle$ (or density matrix method). Prior to the calculation of the polarization $P(\omega)$, a unitary transformation has been used to remove the phase of the optical transition term. The renormalized energy levels of the electron and hole become $\epsilon_e = E_e - \omega/2$ and $\epsilon_h = E_h - \omega/2$. Furthermore, the hopping terms between the leads and dot, $V_{j=L,R;\mathbf{k}}(t) = V_{j=L,R;\mathbf{k}} \exp -(\pm i\omega t)/2$ become time dependent, in which the energy and time dependence of the coupling are factorized. This factorization leads to time-independent tunneling rates and it simplifies the calculation. Solving the equation of motion for $G^<_{eh}(t,t) = -i\langle a^\dagger(t) d_{h,-\sigma}(t) d_{e,\sigma}(t) \rangle$ and considering the steady-state condition, we obtain the lesser Green's function

$$G_{eh}^{<}(\omega)=\frac{-\lambda\mathcal{F}-(U_e-U_{eh})\mathcal{P}_1(\omega)-(U_h-U_{eh})\mathcal{P}_2(\omega)}{\epsilon_e+\epsilon_h-U_{eh}+i\frac{\Gamma}{2}}, \tag{16}$$

where

$$\mathcal{F}=\langle\Phi|a^{\dagger}a|\Phi\rangle(1-N_{e,\sigma}-n_{h,-\sigma})-N_{e,\sigma}n_{h,-\sigma}, \tag{17}$$

$\Gamma\equiv\Gamma_e+\Gamma_h$, which leads to a broadening of the spectrum, and $|\Phi\rangle$ denotes a photon state. $\mathcal{P}_1(\omega)$ and $\mathcal{P}_2(\omega)$ are given by

$$\mathcal{P}_1(\omega)=-\lambda\mathcal{F}N_{e,-\sigma}\left(\frac{1-n_{h,\sigma}}{\epsilon_e+\epsilon_h+U_e-2U_{eh}+i\frac{\Gamma}{2}}+\frac{n_{h,\sigma}}{\epsilon_e+\epsilon_h+U_e+U_h-3U_{eh}+i\frac{\Gamma}{2}}\right) \tag{18}$$

and

$$\mathcal{P}_2(\omega)=-\lambda\mathcal{F}n_{h,\sigma}\left(\frac{1-N_{e,-\sigma}}{\epsilon_e+\epsilon_h+U_h-2U_{eh}+i\frac{\Gamma}{2}}+\frac{N_{e,-\sigma}}{\epsilon_e+\epsilon_h+U_e+U_h-3U_{eh}+i\frac{\Gamma}{2}}\right). \tag{19}$$

The first term in the filling factor $\mathcal{F}$ [Eq. (17)] arises from the stimulated process, which vanishes in the vacuum state. The second term, $N_{e,\sigma}n_{h,-\sigma}$ is due to the spontaneous emission process. This is a quantum effect of the electromagnetic field. Equations (18) and (19) are derived, respectively, from the equation of motion for

$$-i\langle a^{\dagger}(t)N_{e,-\sigma}(t)d_{h,-\sigma}(t)d_{e,\sigma}(t)\rangle$$

and

$$-i\langle a^{\dagger}(t)n_{h,\sigma}(t)d_{h,-\sigma}(t)d_{e,\sigma}(t)\rangle,$$

which are coupled with

$$-i\langle a^{\dagger}(t)n_{h,\sigma}(t)N_{e,-\sigma}(t)d_{h,-\sigma}(t)d_{e,\sigma}(t)\rangle.$$

The term $-i\langle a^{\dagger}(t)N_{e,-\sigma}(t)d_{e,\sigma}(t)d_{h,-\sigma}(t)\rangle$ describes an electron-screened electron-hole recombination process in a negative trion. Similarly, $-i\langle a^{\dagger}(t)n_{h,\sigma}(t)d_{h,-\sigma}(t)d_{e,\sigma}(t)\rangle$, describes a hole-screened electron-hole recombination process in a positive trion, and $-i\langle a^{\dagger}(t)n_{h,\sigma}(t)N_{e,-\sigma}(t)d_{e,\sigma}(t)d_{h,-\sigma}(t)\rangle$ describes the biexciton-to-exciton transition process. In the photon vacuum state, we obtain

$$\mathcal{P}(\omega)/(N_{e,\sigma}n_{h,-\sigma})=\lambda^2\left(\frac{(1-N_{e,-\sigma})(1-n_{h,\sigma})}{E_g-U_{eh}-\omega+i\Gamma/2}+\frac{(1-n_{h,\sigma})N_{e,-\sigma}}{E_g+U_e-2U_{eh}-\omega+i\Gamma/2}+\frac{(1-N_{e,-\sigma})n_{h,\sigma}}{E_g+U_h-2U_{eh}-\omega+i\Gamma/2}+\frac{N_{e,-\sigma}n_{h,\sigma}}{E_g+U_h+U_e-3U_{eh}-\omega+i\Gamma/2}\right). \tag{20}$$

The spectrum of the polarization $\mathcal{P}(\omega)$ displays four peaks, which are attributed to the exciton X, negative trion X^-, positive trion X^+ and biexciton X^2 (biexciton decaying to exciton). The corresponding peak positions occur at $\omega=E_g-U_{eh}$, $\omega=E_g+U_e-2U_{eh}$, $\omega=E_g+U_h-2U_{eh}$ and $\omega=E_g+U_e+U_h-3U_{eh}$, which are significantly influenced by the particle Coulomb interactions.

IV. ENERGY LEVELS AND INTERPARTICLE INTERACTIONS

According to Eqs. (12) and (20), particle Coulomb interactions will significantly affect the tunneling current of SET and the emission spectrum of single photons. To illustrate this effect, we apply our theory to a pyramid-shaped InAs/GaAs QD. First, we calculate the interparticle Coulomb interactions using a simple but realistic effective-mass model. The electronic structures of InAs/GaAs QDs have been extensively studied by several groups with different methods.[31–35] The electron (hole) in the QD is described by the equation

$$\left(-\nabla\frac{\hbar^2}{2m_{e(h)}^{*}(\rho,z)}\nabla+V_{\mathrm{QD}}^{e(h)}(\rho,z)\mp eFz\right)\psi_{e(h)}(\mathbf{r})=E_{e(h)}\psi_{e(h)}(\mathbf{r}), \tag{21}$$

where $m_e^{*}(\rho,z)$ (a scalar) denotes the position-dependent electron effective mass, which has $m_{eG}^{*}=0.067m_e$ for GaAs and $m_{eI}^{*}=0.04m_e$ for the strained InAs in the QD. $m_h^{*}(\rho,z)$ denotes the position-dependent effective mass tensor for the hole. It is a fairly good approximation to describe $m_h^{*}(\rho,z)$ in InAs/GaAs QD as a diagonal tensor with the x and y components given by $m_t^{*-1}=(\gamma_1+\gamma_2)/m_e$ and the z component given by $m_l^{*-1}=(\gamma_1-2\gamma_2)/m_e$. γ_1 and γ_2 are the Luttinger parameters. Their values for InAs and GaAs are taken from Ref. 35. $V_{\mathrm{QD}}^{e}(\rho,z)$ [$V_{\mathrm{QD}}^{h}(\rho,z)$] is approximated by a constant potential in the InAs region with value determined by the conduction-band (valence-band) offset and the deformation potential shift caused by the biaxial strain in the QD. These values have been determined by comparison with results obtained from a microscopic model calculation[31] and we have $V_{\mathrm{QD}}^{e}=-0.5$ eV and $V_{\mathrm{QD}}^{h}=-0.32$ eV. The eFz term in Eq. (21) arises from the applied voltage, where F denotes the strength of the electric field. Using the eigenfunctions of Eq. (21), we calculate the interparticle Coulomb interactions via

$$U_{i,j}=\int d\mathbf{r}_1\int d\mathbf{r}_2\frac{e^2[n_i(\mathbf{r}_1)n_j(\mathbf{r}_2)]}{\epsilon_0|\mathbf{r}_1-\mathbf{r}_2|}, \tag{22}$$

where $i(j)=e$, h, $n_i(\mathbf{r}_1)$ denotes the charge density, and ϵ_0 is the static dielectric constant of InAs. We have ignored the image force arising from the small difference of dielectric constant between InAs and GaAs. Although the Coulomb energies are different in different exciton complexes, their

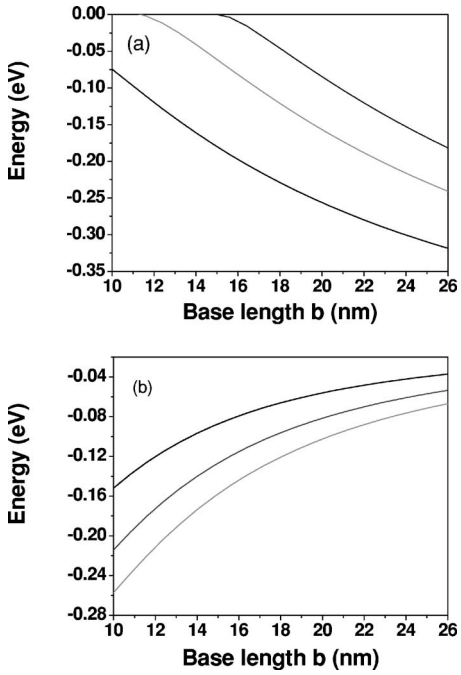

FIG. 2. Lowest three energy levels of a quantum dot as functions of the QD size b for (a) electrons and (b) holes.

difference is rather small.[28,29] Therefore, only one set of Coulomb interaction parameters has been used in this study.

For the purpose of constructing the approximate wave functions, we place the system in a large confining cubic box with length L. Here we adopt $L=40$ nm. The wave functions are expanded in a set of basis functions, which are chosen as sine waves

$$\psi_{nlm}(\rho,\phi,z)=\frac{\sqrt{8}}{\sqrt{L^3}}\sin(k_l x)\sin(k_m y)\sin(k_n z), \qquad (23)$$

where $k_n=n\pi/L, k_m=m\pi/L, k_\ell=\ell\pi/L$. n, m, and ℓ are positive integers. The expression of the matrix elements of the Hamiltonian of Eq. (21) can be readily obtained. In our calculation $n=20$, $m=10$, and $\ell=10$ are used in solving Eq. (21). Figure 2 shows the lowest three energy levels of the pyramidal InAs/GaAs QD as a function of QD size. The ratio of height and base length is fixed at $h/b=1/4$, while h varies from 2.5 to 6.5 nm. Diagrams (a) and (b) denote, respectively, the energy levels for electrons and holes. We can see that the energy level spacing between the ground state and the first excited state is much larger than $k_BT=2$ meV, which will be considered throughout this article. Therefore, the lowest energy levels, E_e and E_h, are adopted in the Hamiltonian of Eq. (1). The intralevel Coulomb interactions U_e and U_h and interlevel Coulomb interaction U_{eh} are calculated using Eq. (22). Figure 3 shows the interparticle interactions as functions of QD size. The strengths of Coulomb interactions are inversely proportional to the QD size. However as the QD size decreases below a threshold value (around $b=12$ nm), U_e is significantly reduced due to the leak out of electron density for small QDs. These Coulomb interactions approach approximately the same value in the large QD limit. This indicates similar degree of localization for electron and hole in large QDs. We also note that U_{eh} is smaller than U_e in the large QD. This is due to the fact that in large QDs the degree of localization for the hole becomes similar to that for electron, while the anisotropic nature of hole wave function reduces U_{eh}. The repulsive Coulomb interactions, U_e and U_h, are the origin of Coulomb blockade for electrons and holes, respectively. The attractive Coulomb interaction U_{eh} gives rise to the binding of the exciton. To study the behavior of tunneling current and bias-dependent spontaneous emission spectrum, we consider a particular pyramidal InAs/GaAs QD with base length $b=13$ nm and height $h=3.5$ nm. The other relevant parameters for this QD are $E_{e,0}=-0.14$ eV, $E_{h,0}=-0.125$ eV, $U_e=16.1$ meV, $U_{eh}=16.7$ meV, and $U_h=18.5$ meV.

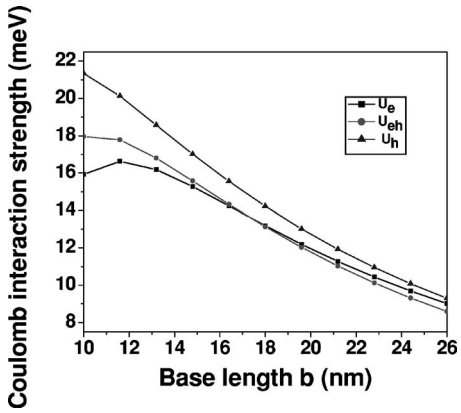

FIG. 3. Intralevel Coulomb interactions U_e and U_h and interlevel Coulomb interaction U_{eh} as functions of the QD base length b.

V. RESULTS

In this section, we discuss our numerical results for the tunneling current and spontaneous emission spectrum. For simplicity, we assume that the tunneling rate $\Gamma_L=\Gamma_R=0.5$ meV is bias independent. We apply a bias voltage V_a across the source-drain and V_g across the gate-drain. With the applied voltages, the QD electron and hole energy levels will be shifted to $E_e+\alpha eV_a-\beta eV_g$ and $E_h+\alpha eV_a-\beta eV_g$, respectively. In our calculation, we assume $\alpha=0.5$ and $\beta=0.7$. Meanwhile the chemical potentials of the electrodes corresponding to a Fermi energy $E_F=60$ meV (relative to the conduction band minimum in the leads) are assumed to be 70 meV below the energy level of E_e at zero bias. Other parameters adopted are: $\Gamma_h=0.2$ meV and $R_{eh}=10$ μeV.

A. Effects of optical pumping on the tunneling current

Applying Eqs. (3), (13), and (15), we solve for the electron occupation number $N_e=N_{e,\sigma}=N_{e,-\sigma}$ and the tunneling current J. Figure 4 shows the calculated results for N_e and J as functions of gate voltage with and without photoexcitation at zero temperature and $V_a=2$ mV. Solid line and dashed line correspond to $I=0$ (no pump) and $I=0.9$ (with pump), respectively. Here I is a dimensionless quantity, defined as I

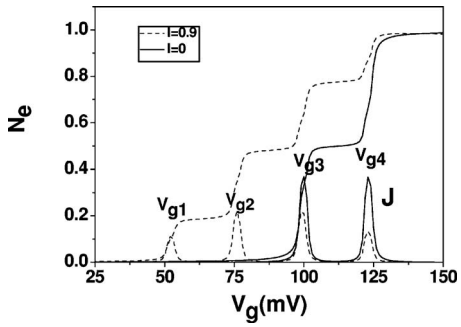

FIG. 4. Electron occupation number N_e and tunneling current as functions of gate voltage at zero temperature for various strengths of optical excitation. Current density is in units of $J_0=2e\times$meV/h.

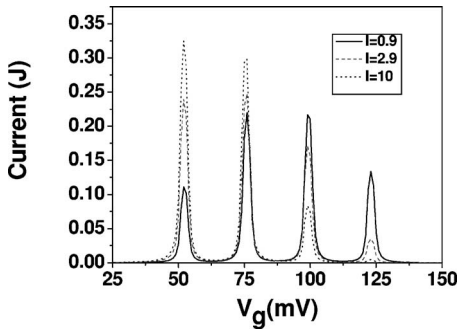

FIG. 5. Tunneling current as a function of gate voltage at zero temperature for various strengths of optical excitation.

$\equiv \gamma_{h,c}N_{h,\mathbf{k}}/\Gamma_{h,s}$ which is proportional to the pump power. The electron occupation number displays several plateaus, while the tunneling current displays an oscillatory behavior. Both are typical behaviors due to the Coulomb blockade. The manipulation of gate voltage can tune the energy levels of the QD. For the no-pump case ($I=0$), carriers in the emitter electrode are allowed to tunnel into the QD as the gate voltage exceeds the threshold voltage, $V_{g3}(\approx 100$ mV). When the energy level of $E_e+\alpha V_a-\beta V_g$ is below the emitter chemical potential, but $E_e+\alpha V_a-\beta V_g+U_e$ above the emitter chemical potential, N_e (for a given spin) reaches 0.5 and displays a plateau which is caused by the Coulomb blockade associated with U_e (the charging energy of the electron ground state). At higher gate voltage, $E_e+\alpha V_a-\beta V_g+U_e$ moves below the emitter chemical potential, and N_e approaches 1. When electron-hole pairs are generated due to optical pumping in addition to the tunneling electrons, various exciton complexes such as the exciton, positive and negative trions, and biexciton can be formed. These new channels allow carriers in the emitter electrode to tunnel into the QD at lower gate voltage. When the gate voltage is below V_{g2}, but above V_{g1}, only the positive trion state is below the emitter chemical potential, hence only a small plateau is seen. As the gate voltage increases, more exciton complex levels are depressed below the emitter chemical potential, and a series of plateaus appear. The value of N_e depends on which exciton complex state is filled and on the pumping intensity.

The tunneling current as a function of the gate voltage can be measured directly. We see that optical pumping leads to two additional peaks below the threshold voltage V_{g3}, which is caused by the electron tunneling assisted by the presence of a hole in the QD. This interesting phenomenon was observed by Fujiwara *et al.* in a SET composed of one silicon QD and three electrodes.[36] The behavior of the photoinduced tunneling current can be understood by analyzing the energy poles of the retarded Green's function as given in Eq. (12). In Fig. 4, the first peak of the dashed line is caused by a resonant tunneling through the energy pole at $\epsilon=E_e-2U_{eh}$ (which corresponds to a positive trion state) with probability $(1-N_{e,-\sigma})(n_{h,\sigma}n_{h,-\sigma})$. The second peak is caused by a pair of poles at $\epsilon=E_e-U_{eh}$ (the exciton state) and $\epsilon=E_e+U_e-2U_{eh}$ (the biexciton state) with probabilities $(1-N_{e,-\sigma})(n_{h,\sigma}+n_{h,-\sigma}-2n_{h,\sigma}n_{h,-\sigma})$ and $N_{e,-\sigma}(n_{h,\sigma}n_{h,-\sigma})$. Since the magnitude of U_e is very close to that of U_{eh} for the present case, the corresponding two peaks merge into one. For other cases (e.g., smaller QDs), the difference between U_e and U_{eh} may be large enough for the peaks to be distinguished. The third peak is caused by another pair of poles at $\epsilon=E_e$ (the single-electron state) and $\epsilon=E_e+U_e-U_{eh}$ (the negative trion state) with probabilities $(1-N_{e,\sigma})[1-(n_{h,\sigma}+n_{h,-\sigma})+n_{h,\sigma}n_{h,-\sigma}]$ and $N_{e,-\sigma}(n_{h,\sigma}+n_{h,-\sigma}-2n_{h,\sigma}n_{h,-\sigma})$. The last peak located near $V_g=123$ mV is due to the resonant tunneling through the energy level at the pole $\epsilon=E_e+U_e$ (the two-electron state) with probability $N_{e,-\sigma}[1-(n_{h,\sigma}+n_{h,-\sigma})+n_{h,\sigma}n_{h,-\sigma}]$. Obviously, the relative strengths of these tunneling current peaks are influenced by the hole occupation numbers. The gate voltage differences $\Delta V_{g21}=V_{g2}-V_{g1}$ and $V_{g43}=V_{g4}-V_{g3}$ allow the determination of the electron–hole interaction and the electron–electron Coulomb repulsion, since $\beta\Delta V_{g21}=U_{eh}$ and $\beta V_{g43}=U_e$. Consequently, such a measurement can be used to determine the exciton binding energy, which is otherwise not possible via typical photoluminescence or the electrically driven emission spectrum measurement. In such a measurement, it is necessary to distinguish U_{eh} from U_e. Thus, we recommend using a smaller bias (V_a), which would make the tunneling peaks sharper and the double-peak features at $V_g=V_{g2}$ and $V_g=V_{g3}$ better resolved.

Figure 5 shows the tunneling current as a function of gate voltage for various strengths of photoexcitation power at zero temperature. According to the definition of $\gamma_{e(h),c}=-\Sigma_{\mathbf{q}}|g_{e(h),\mathbf{q}}|^2 Im\, 1/[\gamma_{e(h),s}(\Omega_{\mathbf{q}}+i\gamma_{e(h),s})]$, the condition $\Gamma_L=\Gamma_R \gg \gamma_{e,c}$ is still satisfied, even though we tune $I=\gamma_{h,c}N_{h,\mathbf{k}}/\Gamma_{h,s}$ up to 10 in Fig. 5. $I=10$ can be regarded as increasing p_{exc} by 10 times, but it is still in the weak pumping regime. We notice that increasing photoexcitation power tends to suppress the tunneling current at high gate voltage. For instance, the peak located at $V_g=123$ mV almost vanishes due to the much reduced probability for the pole at $\epsilon=E_e+U_e$. Based on the results of Figs. 4 and 5, we see that the SET has potential application as an optically controlled switch. For practical applications, we must consider the behavior of the tunneling current for a SET operated at finite temperatures. Figure 6 shows a comparison of the electron occupation number and tunneling current at zero temperature and finite temperature ($k_BT=2$ meV). We see that the plateaus become broadened and the magnitude of the tunneling current peak is reduced as the temperature increases. Thus, a large charging energy is required for SETs to be operated at

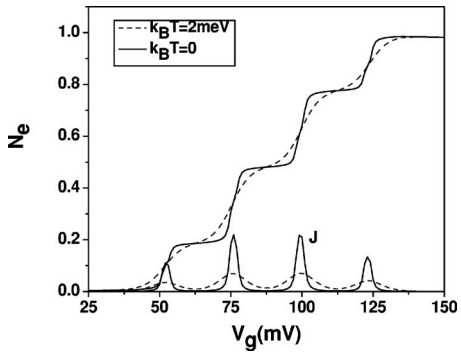

FIG. 6. Electron occupation number N_e and tunneling current as functions of gate voltage for various temperatures at fixed optical excitation strength (I=0.9). Current density is in units of $J_0=2e\times$meV/h.

high temperatures. The tunneling current as a function of applied bias (V_a) for various strengths of photoexcitation power at k_BT=2 meV and V_g=0 is shown in Fig. 7. The tunneling current exhibits a staircase behavior. This is the well-known Coulomb blockade effect. The effect of the optical pumping is to reduce the threshold voltage and increase the number of plateaus in the $J-V$ characteristics. We also notice that a negative differential conductance occurs at high voltages when the resonance level of the QD is below the conduction band minimum of the emitter electrode.

B. Effects of electrodes on the spontaneous emission spectrum

SET has been considered as a single-photon generater (SPG)[27] for quantum information application such as quantum cryptography and teleportation.[37] Thus, it is of great interest to study the spontaneous single-photon emission spectrum of the SET. We previously reported the theoretical studies of the emission spectrum of a single QD embedded in a p-n junction.[28,29] Here, we consider the single-photon emission of a SET (a QD embedded in an n-i-n junction) under optical pumping. Since the magnitudes of interparticle Coulomb interactions U_e, U_h, and U_{eh} are fairly close, it will be difficult to resolve the peaks of exciton (X), negative trion (X^-), positive trion (X^+) and biexciton (X^2) for the case of large tunneling rate as we considered above ($\Gamma_L=\Gamma_R$

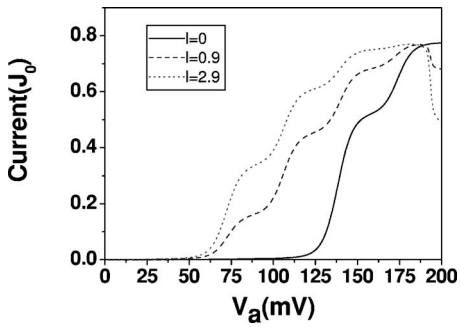

FIG. 7. Tunneling current as a function of applied bias at temperature k_BT=2 meV for various strengths of optical excitation. Current density is in units of $J_0=2e\times$meV/h.

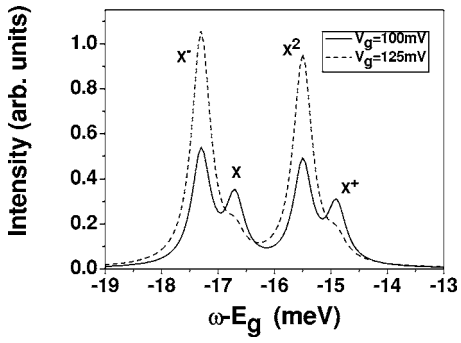

FIG. 8. Intensities of emission spectrum for various gate voltages at fixed optical excitation strength (I=0.9).

=0.5 meV). Therefore, for this study we adopt a small tunneling rate, $\Gamma_L=\Gamma_R=0.1$ meV in order to resolve these peaks in the emission spectrum. This can be achieved, for example, by increasing the barrier thickness between the QD and the conducting leads. Figure 8 shows the emission spectrum for various gate voltages at fixed pump power (I=0.9). For V_g =100 mV, the calculated spontaneous emission spectrum displays four peaks corresponding to X^-, X, X^2, and X^+. The redshift of the X^- peak relative to the exciton peak agrees well with experimental observations.[16,22,24,38] The biexciton peak displaying a blueshift with respect to the exciton peak (showing an antibinding biexciton) is also consistent with the observation reported in Refs. 14 and 19–21. Recently, studies of the binding and antibinding of biexcitons were reported in Ref. 21. Our calculation given by Eqs. (21) and (22) provides only the antibinding feature of biexciton. In Ref. 21 it is pointed out that the biexciton complex changes from antibinding to binding as the QD size increases. For QDs with dimensions larger than the exciton Bohr radius (around 20 nm), the correlation energy becomes significant. In this study, we have not taken into account the correlation energy. This is justified as long as we restrict ourselves to QDs with size less than 20 nm. We see in this figure when the gate voltage is increased up to V_g=125 mV, only the X^- and X^2 peaks survive in the emission spectrum as N_e approaches 1. Furthermore, we can adjust the intensity of excitation power to either enhance or suppress the strength of the biexciton peak. Thompson *et al.* demonstrated that the single photon generated by the biexciton state is significantly less in emission time than the single exciton state.[19] From this point of view, the biexciton state is favored for the application of single-photon generation. We find that one can increase the pump power in order to select the biexciton state as the desired source to produce the single-photon emission. This is demonstrated in Fig. 9, where the emission spectra for various strengths of excitation power at the fixed gate voltage V_g=125 mV are shown. We see that the negative trion saturates at I=1.9 and diminishes afterwards, while the biexciton peak increases quadratically with I and becomes the dominant peak in the emission spectrum.

Finally, we discuss the emission spectrum of an isolated charge-neutral QD with $\Gamma_L=\Gamma_R=0$. For this case the rate equation of exciton number $N_{X,\sigma}$ can be readily obtained by solving the rate equation

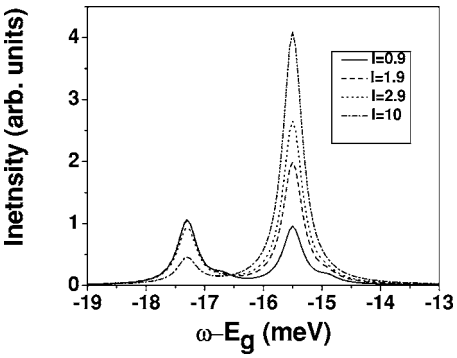

FIG. 9. Intensities of emission spectrum for various strengths of optical excitation at fixed gate voltage (V_g=125 mV).

$$\gamma_{X,c}N_k(1-N_{X,\sigma})-\Omega\int\frac{d\omega}{\pi}\omega\rho(\omega)|ImP(\omega)|=0 \quad (24)$$

with

$$P(\omega)=N_{X,\sigma}\left(\frac{1-N_{X,-\sigma}}{E_X-\omega+i\Gamma/2}+\frac{N_{X,-\sigma}}{E_X+\Delta E_{X,c}-\omega+i\Gamma/2}\right), \quad (25)$$

where $\Omega=4\pi n_r^3\mu_r^2/(6c^3\hbar^3\epsilon_0)$ and n_r is the refractive index of the system. $\rho(\omega)=\omega^2$ arises from the density of states of photons. E_X and $\Delta E_{X,c}$ denote, respectively, the exciton energy and exciton-exciton correlation energy. $\gamma_{X,c}$ denotes the capture rate for excitons from the wetting layer to the QD. After the integration of ω in Eq. (24), we obtain

$$\Omega N_{X,\sigma}[(1-N_{X,-\sigma})E_X^3+N_{X,-\sigma}(E_X+\Delta E_c)^3] \quad (26)$$

for small Γ, and

$$N_{X,\uparrow}=N_{X,\downarrow}=\frac{\gamma_{X,c}N_k}{\gamma_{X,c}N_k+\gamma_{X,r}}, \quad (27)$$

where $\gamma_{X,r}=\Omega E_X^3$ denotes the exciton decaying rate, and we have ignored $\Delta E_{X,c}$, since it is small compared to E_X. According to Eq. (25), we see that the intensities of exciton and biexciton peaks are proportional to $p_{\rm exc}$ and $p_{\rm exc}^2$, if $N_{X,\sigma}$ is proportional to $p_{\rm exc}$ (the excitation power). This is in very good agreement with many experimental reports.[17,19–21,39] Note that in some experiments, the pump energy is far above the QD band gap and the emission occurs after the electrons and holes are captured. This situation becomes similar to the open system considered in the SET with optical pumping. In this case, we can replace $N_{e,\sigma}$ in Eq. (20) by $n_{e,\sigma}$, the electron occupation due to optical pumping, and we can still prove that the intensities of X and X^2 peaks as functions of the excitation power are described by Eqs. (14), (15), and (20). Thus, they exhibit linear and quadratic behavior as a function of $p_{\rm exc}$, respectively. So, there is no qualitative difference between Eq. (20) and Eq. (24) regarding the behavior of X and X^2, except that Eq. (20) also describes the possibility of emission due to recombination in trions. This provides an explanation to the experimental observation of Ref. 17, in which the pump energy is far above the QD band gap and both X^- and X^+ peaks (in addition to the X and X^2 peaks) were observed in the emission spectrum.

VI. SUMMARY

In this article we have studied the tunneling current and emission spectrum of a SET under optical pumping theoretically. We apply our theoretical analysis to a SET, which consists of a single quantum dot embedded in an *n-i-n* junction. We use a simple but realistic effective mass model to calculate the interparticle Coulomb interactions of pyramid-shaped InAs/GaAs QDs. These Coulomb interactions are essential for the study of optical and transport properties of QDs. The retarded Green's function was calculated via a nonequilibrium Green's function method. It is found that the holes in QD generated by optical pumping leads to new channels for electrons to tunnel from the emitter to the collector, which creates a variety of ways to control both the electrical and optical signals. The binding energy of exciton complexes as well as electron charging energy can be determined by examining the tunneling current as a function of gate voltage V_g with a small applied bias V_a. In addition, the emission spectrum of SET can be modified significantly by adjusting bias voltage, the gate voltage, or the pump intensity.

ACKNOWLEDGMENTS

This work was supported by National Science Council of Republic of China under Contract Nos. NSC 93-2215-E-008-014, NSC-93-2120-M-008-002, and NSC 93-2215-E-008-011.

APPENDIX A

In the system described by Eq. (1), electromagnetic field of frequency ω_0 is used to resonantly pump carriers into the InAs wetting layer. Therefore, electrons can be injected into the InAs QD via either the tunneling process or carrier capture from the wetting layer. On the other hand, holes in InAs QD are provided only by the capture process. The dominant carrier capture process is the the optical-phonon assisted carrier relaxation as described by the fifth term in Eq. (1). Due to the discrete density of states in QDs, a phonon bottleneck effect, which leads to the suppression of carrier relaxation rate, has been predicted for QDs.[40] Experimental observation of phonon bottleneck effect was reported by Urayama *et al.*[41] The phonon-assisted capture rate depends on the energy levels and the size of QDs. For the size of QDs considered in our case, the electron capture rate $\gamma_{e,c}$ is estimated to be around 10/ns. Consequently, the condition $\Gamma_e \gg \gamma_{e,c}$ is usually satisfied, where Γ_e denote the electron tunneling rate. Based on the above condition, we can ignore the electron capture process in the calculation of the tunneling current. The tunneling current from the left electrode to the InAs QD can be calculated from the time evolution of the occupation number, $N_L=\Sigma_{\mathbf{k},\sigma;L}c^\dagger_{\mathbf{k},\sigma;L}c_{\mathbf{k},\sigma;L}$.

Prior to the calculation of tunneling current, a unitary transformation is employed to remove the phase of the optical transition term of QD. The renormalized energy levels of

the electron and hole become $\epsilon_e = E_e - \omega/2$ and $\epsilon_h = E_h - \omega/2$. Furthermore, the hopping terms between the leads and the dot become time dependent, $V_{\mathbf{k},j}(t) = V_{\mathbf{k}} \exp[-(\pm i\omega t)/2]$. Now, we can apply the formulas given in Ref. 5. We obtain

$$J = \frac{-2e}{\hbar} \int \frac{d\epsilon}{2\pi} \Gamma_L(\epsilon) \left(\frac{1}{2} G^<_{e,\sigma}(\epsilon) + f_L(\epsilon) Im G^r_{e,\sigma}(\epsilon) \right), \tag{A1}$$

where $\Gamma_L(\epsilon) = 2\pi \Sigma_{\mathbf{k}} |V_{L,\mathbf{k}}|^2 \delta(\epsilon - \epsilon_{\mathbf{k}})$, and $f_L(\epsilon)$ is the Fermi distribution function. $G^<_{e,\sigma}(\epsilon)$ and $G^r_{e,\sigma}(\epsilon)$ are the Fourier transformation of the lesser Green function $G^<_{e,\sigma}(t) = i\langle d^\dagger_{e,\sigma}(0) d_{e,\sigma}(t)\rangle$ and retarded Green's function $G^r_{e,\sigma}(t) = -i\theta(t)\langle [d_{e,\sigma}(t), d^\dagger_{e,\sigma}(0)]\rangle$. Applying Dyson's equation, we obtain

$$G^<_{e,\sigma}(\epsilon) = f^<(\epsilon)[G^r_{e,\sigma}(\epsilon) - G^a_{e,\sigma}(\epsilon)] \tag{A2}$$

with

$$f^<(\epsilon) = \frac{i\sum_{\mathbf{k},\ell} |V_{\mathbf{k},\ell}|^2 g^<_{e,\mathbf{k},\sigma;\ell}(\epsilon) + i\sum_{Q} |\lambda|^2 \mathcal{G}^<_{h,-\sigma}(\epsilon)}{-i\sum_{\mathbf{k},\ell} |V_{\mathbf{k},\ell}|^2 [g^r_{e,\mathbf{k},\sigma;\ell}(\epsilon) - g^a_{e,\mathbf{k},\sigma;\ell}(\epsilon)] - i\sum_{Q} |\lambda|^2 Im\mathcal{G}^r_{h,-\sigma}(\epsilon)}, \tag{A3}$$

where $g^<_{e,\mathbf{k},\sigma;\ell}(\epsilon) = f_\ell(\epsilon)[g^r_{e,\mathbf{k},\sigma;\ell}(\epsilon) - g^a_{e,\mathbf{k},\sigma;\ell}(\epsilon)] \cdot [g^r_\ell(\epsilon) - g^a_\ell(\epsilon)] = i2\pi\delta(\epsilon - \epsilon_{\mathbf{k}})$. The lesser Green's function and retarded Green's function for holes are denoted by $\mathcal{G}^<_{h,-\sigma}(\epsilon)$ and $\mathcal{G}^r_{h,-\sigma}(\epsilon)$. Due to the small electron-hole recombination rate $R_{eh} \approx 1/\text{ns}$, terms involving $|\lambda|^2$ can be dropped [that is to ignore the photocurrent in Eq. (A1)]. After rewriting $f^<(\epsilon)$ as

$$f^<(\epsilon) = -\frac{\Gamma_L(\epsilon) f_L(\epsilon) + \Gamma_R(\epsilon) f_R(\epsilon)}{\Gamma_L(\epsilon) + \Gamma_R(\epsilon)}, \tag{A4}$$

and substituting it into Eq. (A1), we obtain the tunneling current

$$J = \frac{-2e}{\hbar} \int \frac{d\epsilon}{2\pi} \frac{\Gamma_L(\epsilon)\Gamma_R(\epsilon)}{\Gamma_L(\epsilon) + \Gamma_R(\epsilon)} [f_L(\epsilon) - f_R(\epsilon)] Im G^r_{e,\sigma}(\epsilon). \tag{A5}$$

The expression of Eq. (A5) was also obtained by Meir, Wingreen, and Lee.[6] It is of no surprise that we reproduce their result, because the system considered here reduces to their case as the carrier relaxation process and electron-hole recombination process are both turned off. Note that the retarded Green's function $G^r_{e,\sigma}(\epsilon)$ includes the full effects due to the electron–electron Coulomb interaction and electron–hole Coulomb interaction and the effect due to the dot-electrodes coupling. Also note that the electrodes are coupled to the conduction band of the QD, but not to the valence band of the QD.

APPENDIX B

When light is used to resonantly create electrons and holes in the wetting layer, electrons and holes can relax to the InAs QD via optical phonon-assisted process. When electrons relax into InAs QD, they will tunnel out quickly since the electrons in the ground state of the InAs QD are coupled with the electrodes. However, holes in the InAs QD can decay only via recombination with electrons (radiation process) or via impurity scattering (nonradiation process). When holes are present in the InAs QD, we expect the tunneling current to change significantly due to the large electron-hole Coulomb interactions [see Eq. (12)]. In this Appendix, we give the derivations for Eqs. (14) and (15), which describe the electron and hole populations in the InAs QD under optical pumping. First, we introduce the electron and hole distribution functions in the wetting layer, $N_{e,\mathbf{k}} = \langle d^\dagger_{e,\mathbf{k}}(t) d_{e,\mathbf{k}}(t)\rangle$ and $N_{h,-\mathbf{k}} = \langle d^\dagger_{h,-\mathbf{k}}(t) d_{h,-\mathbf{k}}(t)\rangle$. We use the equation-of-motion method to calculate $N_{e,\mathbf{k}} = \langle d^\dagger_{e,\mathbf{k}}(t) d_{e,\mathbf{k}}(t)\rangle$ and $N_{h,-\mathbf{k}} = \langle d^\dagger_{h,-\mathbf{k}}(t) d_{h,-\mathbf{k}}(t)\rangle$. We obtain

$$i\frac{d}{dt} N_{e,\mathbf{k}} = -i\gamma_{e,s} N_{e,\mathbf{k}} + 2Im\langle \lambda^\dagger_0 b^\dagger_{e,\mathbf{k}} b^\dagger_{h,-\mathbf{k}}\rangle - 2\sum_{\mathbf{q}} Im g_{e,\mathbf{q}} \langle A b^\dagger_{e,\mathbf{k}} d_{e,\sigma}\rangle, \tag{B1}$$

and

$$i\frac{d}{dt} N_{h,-\mathbf{k}} = -i\gamma_{h,s} N_{h,-\mathbf{k}} + 2Im\langle \lambda^\dagger_0 b^\dagger_{e,\mathbf{k}} b^\dagger_{h,-\mathbf{k}}\rangle - 2\sum_{\mathbf{q}} Im g_{h,\mathbf{q}} \langle A b^\dagger_{h,-\mathbf{k}} d_{h,-\sigma}\rangle, \tag{B2}$$

where $\gamma_{e(h),s}$ denotes the carrier scattering rate due to mechanisms not considered in the Hamiltonian. $\langle \lambda^\dagger_0 b^\dagger_{e,\mathbf{k}} b^\dagger_{h,-\mathbf{k}}\rangle$ represents the polarization for creating an electron-hole pair in the wetting layer. $g_{e,\mathbf{q}}\langle A b^\dagger_{e,\mathbf{k}} d_{e,\sigma}\rangle$ ($g_{h,\mathbf{q}}\langle A b^\dagger_{h,-\mathbf{k}} d_{h,-\sigma}\rangle$) are terms due to the process for transferring one electron (hole) from the QD to the wetting layer by absorbing one optical phonon. To terminate the equations of motion [Eqs. (B1) and (B2)], we need to solve $\langle \lambda^\dagger_0 b^\dagger_{e,\mathbf{k}} b^\dagger_{h,-\mathbf{k}}\rangle$ and

$$g_{e,\mathbf{q}}\langle A b^\dagger_{e,\mathbf{k}} d_{e,\sigma}\rangle (g_{h,\mathbf{q}}\langle A b^\dagger_{h,-\mathbf{k}} d_{h,-\sigma}\rangle).$$

The equation of motion for $g_{e,\mathbf{q}}\langle A b^\dagger_{e,\mathbf{k}} d_{e,\sigma}\rangle$ leads to

$$\frac{d}{dt}g_{e,\mathbf{q}}\langle Ab^{\dagger}_{e,\mathbf{k}}d_{e,\sigma}\rangle = (i\Omega_q - \gamma_{e,s})g_{e,\mathbf{q}}\langle Ab^{\dagger}_{e,\mathbf{k}}d_{e,\sigma}\rangle + |g_{e,\mathbf{q}}|^2 \cdot$$

$$\{(1+n_q)[1-(n_e+N_e)]N_{e,\mathbf{k}} - n_q(n_e+N_e)(1-N_{e,\mathbf{k}})\}, \tag{B3}$$

where n_q denotes the phonon distribution function, defined as $n_q(\omega_q)=1/[\exp(\omega_q/k_bT)-1]$. $n_e=\langle d^{\dagger}_{e,\sigma}(t)d_{e,\sigma}(t)\rangle_p$ and $N_e=\langle d^{\dagger}_{e,\sigma}(t)d_{e,\sigma}(t)\rangle_t$ denote the electron occupation number of the QD due to the pumping process and tunneling process, respectively, $\Omega_q=(\epsilon_{\mathbf{k}}-E_e-\omega_q)$. Meanwhile, the polarization obeys the following equation

$$\frac{d}{dt}\langle \lambda^{\dagger}_0 b^{\dagger}_{e,\mathbf{k}} b^{\dagger}_{h,-\mathbf{k}}\rangle = (-i\Omega_0 + \gamma_{e,s} + \gamma_{h,s})\langle \lambda^{\dagger}_0 b^{\dagger}_{e,\mathbf{k}} b^{\dagger}_{h,-\mathbf{k}}\rangle - i|\lambda_0|^2(1-N_{e,\mathbf{k}}-N_{h,-\mathbf{k}}), \tag{B4}$$

where $\Omega_0=\epsilon_{e,\mathbf{k}}+\epsilon_{h,-\mathbf{k}}-\omega_0$. In the steady state, we obtain

$$N_{e,\mathbf{k}} = p_{\mathrm{exc}}(1-N_{e,\mathbf{k}}-N_{h,-\mathbf{k}}) - \gamma_{e,c}[(1+n_q)[1-(n_e+N_e)]N_{e,\mathbf{k}} - n_q(n_e+N_e)(1-N_{e,\mathbf{k}})], \tag{B5}$$

where $p_{\mathrm{exc}} \equiv -Im|\lambda_0|^2/\{\gamma_{e,s}[\Omega_0+i(\gamma_{e,s}+\gamma_{h,s})]\}$ and $\gamma_{e,c}=-\Sigma_{\mathbf{q}}\, Im|g_{e,\mathbf{q}}|^2/[\gamma_{e,s}(\Omega_q+i\gamma_{e,s})]$. For low pumping intensity, $N_{e,\mathbf{k}}$ is linearly proportional to p_{exc}. In addition, we note that $\gamma_{e,c}$ is fairly small due to the phonon bottleneck effect of the QD. Similarly for holes in the wetting layer, we obtain

$$N_{h,-\mathbf{k}} = p_{\mathrm{exc}}(1-N_{e,\mathbf{k}}-N_{h,-\mathbf{k}}) - \gamma_{h,c}[(1+n_q)(1-n_h)N_{h,-\mathbf{k}} - n_q n_h(1-N_{h,-\mathbf{k}})], \tag{B6}$$

where $\gamma_{h,c}=-\Sigma_{\mathbf{q}}\, Im|g_{h,\mathbf{q}}|^2/[\gamma_{h,s}(\Omega_q+i\gamma_{h,s})]$ is the hole capture rate. Next, we need to solve the equation of motion for $n_{e,\sigma}$ and $n_{h,-\sigma}$. We have

$$i\frac{d}{dt}n_{e,\sigma} = -i\Gamma_e n_{e,\sigma} + \sum_{\mathbf{Q}} 2Im\langle \lambda^{\dagger} a d^{\dagger}_{e,\sigma} d^{\dagger}_{h,-\sigma}\rangle + 2Img_{e,\mathbf{q}}\langle Ab^{\dagger}_{e,\mathbf{k}}d_{e,\sigma}\rangle, \tag{B7}$$

and

$$i\frac{d}{dt}n_{h,-\sigma} = -i\Gamma_{h,s} n_{h,-\sigma} + \sum_{\mathbf{Q}} 2Im\langle \lambda^{\dagger} d^{\dagger}_{e,\sigma} d^{\dagger}_{h,-\sigma}\rangle + 2Img_{h,\mathbf{q}}\langle Ab^{\dagger}_{h,-\mathbf{k}}d_{h,-\sigma}\rangle, \tag{B8}$$

where $\Gamma_e=\Gamma_L+\Gamma_R$ and $\Gamma_{h,s}$ denote the electron tunneling rate and hole-impurity scattering rate, respectively. At low temperatures, the phonon-absorption process is negligible, since $n_q \to 0$. Using Eqs. (B3) and (20), we obtain the steady-state solution for $n_{e,\sigma}$.

$$n_{e,\sigma} = \frac{\gamma_{e,c}N_{e,\mathbf{k}}(1-N_e)}{\gamma_{e,c}N_{e,\mathbf{k}} + R_{eh}n_h + \Gamma_e}. \tag{B9}$$

Note that the electron-hole recombination rate R_{eh} is given by

$$R_{eh} = \Omega \int \frac{d\omega}{\pi}\rho(\omega)|Im\mathcal{P}(\omega)|, \tag{B10}$$

where $\Omega=4\pi n_r^3\mu_r^2/(6c^3\hbar^3\epsilon_0)$ and n_r is the refractive index of the system. $\rho(\omega)=\omega^2$ arises from the density of states of photons. Similarly, we obtain

$$n_{h,-\sigma} = \frac{\gamma_{h,c}N_{h,\mathbf{k}}}{\gamma_{h,c}N_{h,-\mathbf{k}} + R_{eh}(n_e+N_e) + \Gamma_{h,s}}. \tag{B11}$$

Because of the condition $\Gamma_e \gg \gamma_{e,c}$ and weak pumping intensity, we have $N_{i,\mathbf{k}} \approx p_{\mathrm{exc}}$, and n_e is negligible. As for N_e, we can employ Eqs. (A2) and (A4) to obtain

$$N_{e,\sigma} = -\int \frac{d\epsilon}{\pi}\frac{\Gamma_L f_L(\epsilon) + \Gamma_R f_R(\epsilon)}{\Gamma_L+\Gamma_R} ImG^r_{e,\sigma}(\epsilon). \tag{B12}$$

[1] D. Goldhabar-Gordon, H. Shtrikman, D. Mahalu, D. Abusch-Magder, U. Meirav, and M. A. Kastner, Nature (London) **391**, 156 (1998).

[2] S. M. Cronenwett, T. H. Oosterkamp, and L. P. Kouwenhoven, Science **281**, 540 (1998).

[3] J. H. F. Scott-Thomas, S. B. Field, M. A. Kastner, H. I. Smith, and D. A. Antoniadis, Phys. Rev. Lett. **62**, 583 (1989).

[4] U. Meirav, M. A. Kastner, and S. J. Wind, Phys. Rev. Lett. **65**, 771 (1990).

[5] A. P. Jauho, N. S. Wingreen, and Y. Meir, Phys. Rev. B **50**, 5528 (1994).

[6] Y. Meir, N. S. Wingreen, and P. A. Lee, Phys. Rev. Lett. **70**, 2601 (1993).

[7] H. Haug and A. P. Jauho, *Quantum Kinetics in Transport and Optics of Semiconductor* (Springer, Heidelberg, 1996).

[8] L. Zhuang, L. Guo, and S. Y. Chou, Appl. Phys. Lett. **72**, 1205 (1998).

[9] M. Saitoh, N. Takahashi, H. Ishikuro, and T. Hiramoto, Jpn. J. Appl. Phys., Part 1 **40**, 2010 (2001).

[10] Y. T. Tan, T. Kamiya, D. Zak, and H. Ahmed, J. Appl. Phys. **94**, 633 (2003).

[11] P. W. Li, W. M. Liao, D. M. T. Kuo, S. W. Lin, P. S. Chen, S. C. Lu, and M. J. Tsai, Appl. Phys. Lett. **85**, 1532 (2004).

[12] T. Takagahara and K. Takeda, Phys. Rev. B **46**, 15578 (1992).

[13] P. Michler, A. Kiraz, C. Becher, W. V. Schoenfeld, P. M. Petroff, L. D. Zhang, E. Hu, and A. Imamoglu, Science **290**, 2282 (2000).

[14] Z. Yuan, B. E. Kardynal, R. M. Stevenson, A. J. Shield, C. J. Lobo, K. Cooper, N. S. Beattlie, D. A. Ritchie, and M. Pepper, Science **295**, 102 (2002).

[15] A. Imamoglu and Y. Yamamoto, Phys. Rev. Lett. **72**, 210 (1994).

[16] L. Landin, M. S. Miller, M. E. Pistol, C. E. Pryor, and L. Samuelson, Science **280**, 262 (1998).

[17] C. Santori, M. Pelton, G. Solomon, Y. Dale, and Y. Yamamoto, Phys. Rev. Lett. **86**, 1502 (2001).

[18] C. Santori, D. Fattal, M. Pelton, G. S. Solomon, and Y. Yamamoto, Phys. Rev. B **66**, 045308 (2002).

[19] R. M. Thompson, R. M. Stvenson, A. J. Shields, I. Farrer, C. J.

Lobo, D. A. Ritchie, M. L. Leadbeater, and M. Pepper, Phys. Rev. B **64**, 201302 (2001).
[20] E. Moreau, I. Robert, L. Manin, V. Thierry-Mieg, J. M. Gerard, and I. Abram, Phys. Rev. Lett. **87**, 183601 (2001).
[21] S. Rodt, R. Heitz, A. Schliwa, R. L. Sellin, F. Guffarth, and D. Bimberg, Phys. Rev. B **68**, 035331 (2003).
[22] R. J. Warburton, C. Schaflein, D. Haff, F. Bickel, A. Lorke, K. Karral, J. M. Garcla, W. Schoenfeld, and P. M. Petroff, Nature (London) **405**, 926 (2000).
[23] A. Hogele, S. Seidl, M. Kroner, K. Karrai, R. J. Warburton, B. D. Gerardot, and P. M. Petroff, Phys. Rev. Lett. **93**, 217401 (2004).
[24] F. Findeis, M. Baier, E. Beham, A. Zrenner, and G. Abstreiter, Appl. Phys. Lett. **78**, 2958 (2001).
[25] T. Brandes, Phys. Rep. **408**, 315 (2005).
[26] Y. C. Chang and D. M. T. Kuo, Appl. Phys. Lett. **83**, 156 (2003).
[27] D. M. T. Kuo, Jpn. J. Appl. Phys., Part 2 **43**, L1607 (2004).
[28] D. M. T. Kuo and Y. C. Chang, Phys. Rev. B **69**, 041306 (2004).
[29] D. M. T. Kuo and Y. C. Chang, J. Phys. Soc. Jpn. **74**, 690 (2005).
[30] L. V. Keldysh, Zh. Eksp. Teor. Fiz. **47**, 1515 (1964) [Sov. Phys. JETP **20**, 1018 (1965)].
[31] O. Stier, M. Grundmann, and D. Bimberg, Phys. Rev. B **59**, 5688 (1999).
[32] S. J. Sun and Y. C. Chang Phys. Rev. B **62**, 13631 (2000).
[33] C. Pryor, Phys. Rev. B **57**, 7190 (1998).
[34] L. W. Wang, J. Kim, and A. Zunger, Phys. Rev. B **59**, 5678 (1999).
[35] P. Lawaetz, Phys. Rev. B **4**, 3460 (1971).
[36] A. Fujiwara, Y. Takahashi, and K. Murase, Phys. Rev. Lett. **78**, 1532 (1997).
[37] K. J. Vahala, Nature (London) **424**, 839 (2003).
[38] A. Hartmann, Y. Ducommun, E. Kapon, U. Hohenester, and E. Molinari, Phys. Rev. Lett. **84**, 5648 (2000).
[39] K. Brunner, G. Abstreiter, G. Bohm, G. Trankle, and G. Weimann, Phys. Rev. Lett. **73**, 1138 (1994).
[40] U. Bockelmann and G. Bastards, Phys. Rev. B **42**, 8947 (1990).
[41] J. Urayama, T. B. Norris, J. Singh, and P. Bhattacharya, Phys. Rev. Lett. **86**, 4930 (2001).